Greenhouse Gases and Submarine Groundwater Discharge in a Sydney Harbour Embayment (Australia)

Mahmood Sadat-Noori[1,2*], Douglas R. Tait[1,2], Damien T. Maher[2], Ceylena Holloway[1,2], Isaac R. Santos[1,2]

[1]National Marine Science Centre, School of Environment, Science and Engineering, Southern Cross University, Coffs Harbour, NSW, Australia

[2]School of Environment, Science and Engineering, Southern Cross University, Lismore, NSW, Australia

[*]Corresponding author:

M. Sadat-Noori, School of Environment, Science and Engineering, Southern Cross University, PO Box 157 Lismore, NSW 2480, Australia (mahmood.sadat-noori@scu.edu.au)

Phone: +61 401 816 600

Running head: Greenhouse gases drivers: groundwater or surface water?

Abstract

We investigated whether submarine groundwater discharge (SGD) traced by radon (^{222}Rn, a natural groundwater tracer) may drive carbon dioxide (CO_2), methane (CH_4) and nitrous oxide (N_2O) in surface waters in Chowder Bay, a marine embayment in Sydney Harbour, Australia. A radon mass balance revealed significant groundwater discharge rates into the bay (8.7 ± 5.8 cm d^{-1}). The average CO_2, CH_4, and N_2O concentrations in the subterranean estuary were 3.5, 7.2, and 2.8 times higher than the average surface water concentrations, indicating the possibility of coastal groundwater as a source of greenhouse gases to the bay. SGD-derived fluxes of greenhouse gases were 5.02 ± 2.28 mmol m^{-2} d^{-1}, 5.63 ± 2.55 µmol m^{-2} d^{-1}, and 1.72 ± 0.78 µmol m^{-2} d^{-1} for CO_2, CH_4 and N_2O, respectively. The average CO_2 evasion rate from surface water was 2.29 ± 0.46 mmol m^{-2} d^{-1} while CH_4 and N_2O evasion rates were 12.89 ± 3.05 and 1.23 ± 0.25 µmol m^{-2} d^{-1} respectively. Therefore, groundwater-derived greenhouse gas fluxes accounted for >100% CO_2 and N_2O and ~43% of CH_4 surface water evasion, indicating SGD is likely an important source of greenhouse gases to surface waters. However, this may be due to observations being performed near the SGD source, which may overestimate its contribution to the wider Sydney Harbour. On a 20-year time frame the combined emissions of CH_4 and N_2O from surface waters to the atmosphere accounted for 25% of the total CO_2-equivalent emissions. Although this study gives preliminary insight into SGD and greenhouse gas dynamics in Sydney Harbour, more spatial and temporal resolution sampling is required to fully constrain these processes.

Key Words: Radon, Subterranean Estuary, Greenhouse Gases, Carbon dioxide, Methane, Nitrous oxide, Chowder Bay.

1. Introduction

Coastal ecosystems play an important role in the global carbon cycling with most of the world estuaries being a source of the major greenhouse gases [i.e. carbon dioxide (CO_2), methane (CH_4) and nitrous oxide (N_2O)] to the atmosphere (Borges and Abril, 2011; Bange et al., 1996). Disturbing natural coastal ecosystems and surrounding habitats may lead to significant pollution in waterways and the release of large amounts of buried carbon to the atmosphere (Lovelock et al., 2011; Adame et al., 2013). Previous studies have shown that SGD can deliver significant amounts of nutrients, dissolved carbon and trace metals to coastal waters (Beck et al., 2009; Knee et al., 2011; Porubsky et al., 2014; Lecher et al., 2015). Recently, several studies have suggested that submarine groundwater discharge (SGD) can also deliver large amounts of greenhouse gas into coastal surface waters (O'Reilly et al., 2015; Maher et al., 2015; Sadat-Noori et al., 2016). Solute concentrations, including contaminants, in groundwater are usually higher than in surface marine waters, making groundwater discharge a potentially important driver of surface water chemistry (Santos et al. 2009).

SGD is defined as any water derived by terrestrial and marine forces from the sediment into the surface water column (Moore et al., 2010). Common drivers of SGD are hydraulic head gradient, tidal pumping, and density-driven convection (Santos et al., 2012). Despite increased awareness, SGD remains poorly understood in several environments such as coastal megacities. For example, SGD studies on two major urbanized Asian megacities revealed that SGD-derived dissolved inorganic nitrogen can account for up to 130 and 46% of the rivers nutrient input, demonstrating that SGD should be examined in more detail as an important source of biogeochemically-active elements (Burnett et al., 2007; Taniguchi et al., 2008).

Over the last two decades there has been significant advances in the techniques used to measure natural geochemical tracers which can quantify SGD (Burnett et al. 2006). Radon (^{222}Rn) is natural tracer which has proven to be an effective tool in quantitatively investigating groundwater-surface water interactions. The main advantages of ^{222}Rn is its ability to integrate signals related to different groundwater pathways which may be useful in spatially heterogeneous and temporally dynamic systems (Stieglitz et al., 2010; Burnett et al., 2006). Additionally, ^{222}Rn has conservative behaviour, is highly soluble compared to its radioactive parents, occurs naturally, and has higher concentration in groundwater in comparison to surface waters (Burnett et al. 2006). The short half-life of ^{222}Rn (3.84 days) is

77 advantageous as it is on the same time scale as many physical process related to groundwater
78 discharge and physical mixing of coastal waters (Burnett et al., 2010).
79 The Sydney Harbour Estuary is the centrepiece of Australia's largest city. This iconic
80 waterway has immense social, economic and biological value (Smoothey et al., 2016).
81 Sydney Harbour catchment accommodates approximately one-fifth of Australia's population
82 (4.8 million residents) (Banks et al., 2016), putting the catchment of the estuary under
83 extensive industrial and coastal development pressure (Johnston et al., 2015; Birch et al.,
84 2015). Although Sydney Harbour Estuary has been studied from the marine, biological and
85 ecological perspectives in detail, the majority of these studies have focused on urban runoff
86 (Stark, 1998), stormwater (Birch et al., 2010) and river inputs (Birch et al., 1996; Banks et al.,
87 2016). Several studies on heavy metals within Sydney Harbour indicate benthic sediments are
88 highly contaminated with heavy metals, but much lower concentrations are found in surface
89 waters near the mouth of the estuary (Birch and Taylor 1999; Hatje et al., 2003; Birch et al.,
90 2015). There are no previous studies addressing SGD and related chemical inputs into
91 Sydney Harbour. Additionally, there is a lack of studies investigating hydrologic process
92 within the Harbour and no time series data sets that identify trends and major drivers of biotic
93 interactions (Johnston et al., 2015).
94 This study will, for the first time, quantify submarine groundwater discharge and its
95 associated greenhouse gases (GHG) in an embayment from Sydney Harbour. Visible
96 groundwater seeps around Sydney Harbour led us to hypothesize that SGD may be a major
97 source of water and greenhouse gases to the Harbour. We test this hypothesis by conducting
98 high frequency time series measurements of dissolved CO_2, CH_4 and N_2O in Chowder Bay,
99 Sydney Harbour. We use a well-established groundwater tracer approach utilizing a ^{222}Rn
100 mass balance, to quantify groundwater advection rates and compare SGD-derived fluxes of
101 greenhouse gas to fluxes at the surface water-air interface.
102

103 # 2. Material and methods

104

105 ## 2.1. Site description

106 The study was conducted in Chowder Bay, a small cove in Sydney Harbour, Australia.
107 Sydney Harbour is a heavily industrialized waterway surrounded by the city of Sydney
108 (Figure 1). Sydney Harbour Estuary is ~30 km long, has an average depth of 13 m and is a
109 very productive ecosystem containing a diverse variety of habitats and organisms. The

estuary's upper and central sections are comprised of muddy sediment whereas the lower estuary has sandy bottom sediments (Birch et al., 2008). Estuary flushing times can vary from less than a day at the mouth of the estuary to up to 225 days in the upper parts (Das et al., 2006; Siboni et al., 2016). Chowder Bay is located close to the entrance of Sydney Harbour (33°50′48″S, 151°15′15″E), representing typical marine conditions with some potential influence of urban runoff and inputs from the upper estuary. Although the bay area is protected from dominant south easterly swells it is affected by wind-induced waves and storm swells (Hill et al., 2011). The seafloor is generally sandy with rocky reef outcroppings and gentle slopes (Johnston et al., 2015).

Chowder Bay has an area of about 4300 m^2 and a catchment size of 0.5 km^2. The habitat surrounding Chowder Bay is mainly soft sediments containing some seagrasses (*Zostera capricorni* and *Halophila ovalis*) and shallow fringing rocky reefs (Glasby, 2001). The region receives ~1200 mm of rainfall annually and experiences a mild, warm, temperate climate all year round. Chowder Bay area is located at the low point within its sub-catchment and collects stormwater. The Parramatta River is the main tributary entering Sydney Harbour and has an annual water flux of 473 × 10^5 m^3 (Hatje et al., 2001). During dry weather conditions fresh-water discharge is low (<0.1 m^3 s^{-1} at all discharge locations). Precipitation, freshwater inflow and evaporation are thought to mostly regulate salinity in Sydney Harbour (Lee et al., 2011). During dry periods, the harbour generally has the same salinity as the ocean (~35) and is well mixed. However, after rainfall the mouth of the Harbour can have salinity of about 30 in the upper 1-2 m (Hedge et al., 2014).

2.2. Surface water GHG and ^{222}Rn time series

A field campaign was carried out from 19th to the 23rd November 2015. We deployed an automatic high frequency time series monitoring station on a jetty 80 meters from the shore within Chowder Bay (Figure 1). The station continually monitored water depth, salinity, temperature, dissolved oxygen, pH, fCO_2, pCH_4, N_2O and ^{222}Rn over the duration of the field campaign. Surface water was pumped from 1 meter below the surface at a point where the average water depth was ~5 m. An automated ^{222}Rn monitor (RAD7, Durridge Co.) averaged ^{222}Rn concentrations over 30 minute cycles for about five days. Two cavity ring-down spectrometers (Picarro G2201-i- and G2308) coupled to a showerhead equilibrator were used to measure dissolved CO_2, CH_4 and N_2O at ~ 1 Hz (Maher et al, 2013) with data averaged over 1 minute intervals. Briefly, water was pumped at a constant rate of 3 L m^{-1} to an

equilibrator chamber where the gas in air and water reaches equilibrium. The equilibrated air is then continuously pumped in a closed-loop from the headspace of the equilibrator chamber through desiccant (Drierite), the RAD7 and the Picarros and then back to the equilibrator. The equilibration time for CO_2, CH_4, and ^{222}Rn using this set up is ~ 5 min, 20 min, and 30 minutes respectively (Webb et al., 2016; Santos et al., 2012), with the equilibration time of N_2O assumed to be similar to CO_2 based on their similar solubilities (Arévalo-Martínez et al., 2013). CH_4 and N_2O fugacity were converted to concentrations based on the solubility coefficient calculated as a function of temperature and salinity (Wiesenburg and Guinasso, 1979; Weiss and Price, 1980). The sampling was conducted around neap tide with a tidal range from 0.8 m at the beginning of the campaign and increasing to 1.2 m towards the end (Figure 2). A calibrated Hydrolab (DX5) automatic logger was used to measure salinity (± 0.2), dissolved oxygen (± 0.2 mg L^{-1}) and water temperature (± 0.10 °C) at 15 min intervals while a depth logger (CTD diver) measured depth (± 0.01 m) at 10 min intervals. An Ocean pH Sensor (SAMI) was used to measure pH (± 0.003 units). Wind speed data (± 10%) were obtained from a weather station (Model PH1000) on site.

2.3. Groundwater sampling and analysis

A push point piezometer system was used to collect groundwater samples (Charette and Allen, 2006) across a salinity gradient from the high tide mark to the low tide mark. Shallow wells ranging between 0.5 – 2 m deep were dug on the beach near to the time series station (Figure 1) at low tide. A peristaltic pump was used to take samples after the wells were purged. The tubing was thoroughly flushed with the sample prior to sampling. A calibrated handheld YSI multiprobe was used to measure pH, temperature, DO and salinity for each groundwater sample. Samples for CO_2, CH_4 and N_2O were collected in gas-tight 250 ml bottles. Water was overflowed at least 3 times the bottle volume and 200 µL of saturated $HgCl_2$ solution was added. Samples for groundwater ^{222}Rn analysis were collected in six-litre gas-tight HDPE plastic bottles. Each bottle was connected to a RAD7 radon monitor and given at least 2 hours to achieve an air-water ^{222}Rn equilibrium with <5% uncertainty following well established protocols (Lee and Kim 2006). A total of 10 groundwater samples were collected.

Groundwater CO_2, CH_4 and N_2O samples were analyzed via a headspace method (Gatland et al., 2014). Briefly, 50 mL of sample water was drawn out using a gas syringe fitted with a hypodermic needle head while simultaneously 50 mL of synthetic CO_2, CH_4 and

N_2O-free air was added to the sample. Bottles were then placed on a shaker for 1 min, placed upside down, and left for 18–24 h at room temperature to equilibrate. Thereafter, using a gas syringe, equilibrated air was extracted and 40 mL was expelled into gas tight 0.5 L Tedlar® film bags, while using 10 mL for flushing the lines beforehand. Samples were diluted with 350 mL of atmospheric air before analysis via the G2201-i-I and G2308 Picarros.

2.4. ^{222}Rn ingrowth and diffusion from sediments

To estimate ^{222}Rn molecular diffusion from sediments, three sediment cores were sampled from the study area. Samples were incubated in 60 cm long and 10 cm diameter cylinders. The cores were sealed and incubated with radium free water and left for a period of one month. This experiment was based on the assumption that after a month (>6 half-lives for ^{222}Rn) the only source of ^{222}Rn (diffusion) will reach equilibrium with the only sink (decay) within the core (Santos and Eyre, 2011). The overlying water in the incubation cores was extracted into six-liter gas tight plastic bottles and ^{222}Rn concentration in the water was measured using a RAD7 and closed loop system (Lee and Kim, 2006). The entire water column in each core was sampled from the bottom up preventing any effects of heterogeneity within the core. The diffusion fluxes were used in a ^{222}Rn mass balance to estimate SGD rates.

To assess the ^{222}Rn ingrowth from the decay of its parent isotope, ^{226}Ra, two 80 L containers were filled with water, at low tide, and two 80 L samples were collected at high tide. The water was then passed through a magnesium fibre which quantitatively absorbs the radium from the water (Moore, 2003). The fibres were then sealed and left for at least one month before ^{226}Ra concentration analysis was done using a Radium Delayed Coincidence Counter (RaDeCC) (Peterson et al., 2009). These data were then used as an input to the ^{222}Rn mass balance.

2.6. SGD calculations and GHG fluxes

A non-steady state ^{222}Rn mass balance model was applied to estimate the groundwater discharge rate (cm d^{-1}) into the cove (Burnett and Dulaiova, 2003). Briefly, the model accounts for all sources (i.e. groundwater, diffusion from sediments, ^{226}Ra decay) and sinks (i.e. decay and atmospheric evasion) of ^{222}Rn entering and leaving the system. The model is based on the temporal (hourly) change of ^{222}Rn inventories in surface waters and accounts for ^{222}Rn ingrowth from dissolved ^{226}Ra, ^{222}Rn decay (negligible at 1-hour time steps),

atmospheric evasion losses and mixing with lower concentration offshore waters. In brief, ^{222}Rn concentration in the water column is corrected for ^{222}Rn not supported by ^{226}Ra, then normalized to mean tidal height to remove the effect of changing inventories for each measurement interval (i.e. at flood tide corrections would be negative due to increase in depth and inventory). The tide normalized inventories are then corrected for atmospheric evasion losses for each measurement interval based on the equation described below. Additionally, mixing losses between Chowder Bay and the wider Harbour are estimated based on the rate of decrease of the radon inventory over each tidal cycle assuming the lowest concentrations observed during each mixing cycle (forced to match tidal cycles) represents the Harbour waters (Burnett and Dulaiova, 2003). The model has been widely applied to near-shore environments where no breaking waves are present such as Chowder Bay (e.g. Santos et al., 2009; Dulaiova and Burnett, 2006; Cyronak et al., 2014). Errors regarding the ^{222}Rn mass balance were calculated following the basic rules of error propagation.

Greenhouse gas fluxes derived from SGD (μmol m^{-2} d^{-1}) were then calculated by multiplying the ^{222}Rn-derived SGD rate by the average concentration of the gases in local beach groundwater. Greenhouse gas atmospheric water to air fluxes were calculated using the equations of Wanninkhof (1992):

$$F = k\,\alpha\,(C_{water} - C_{air}) \quad (1)$$

Where F is the flux of CO_2, CH_4 or N_2O in units of mmol m^{-2} d^{-1} , C_{water} and C_{air} are the partial pressure of CO_2, CH_4 or N_2O in the water column and in air, respectively, in units of μatm; The atmospheric pCO_2, pCH_4 and N_2O were assumed to be constant at an average of 400, 1.8 and 0.328 μatm, respectively; α is the solubility coefficient, calculated as a function of temperature and salinity using the constants of Weiss (1974) for CO_2, Weiss, and Price (1980) for N_2O and Wiesenburg and Guinasso, (1979) for CH_4; k is the gas transfer velocity at the water–air boundary (m d^{-1}). The main uncertainty associated with quantifying air-water gas exchange results from the estimation of gas transfer velocity, therefore k was calculated using the wind-speed based parameterization method of five different authors to provide a reasonable range in evasion rates (Wanninkhof, 1992; Crusius & Waninnkhof, 2003; Wanninkhof and McGillis, 1999; Raymond and Cole, 2001; and Borges et al., 2004). The transfer velocity equations rely on wind speeds (U) at a height of 10 m (m s^{-1}), the gas specific Schmidt number (Sc) at in situ temperatures and salinities (Wanninkhof 1992).

Water-to-air GHG fluxes were calculated using the average daily wind speeds collected on the site.

3. Results

3.1. Surface water

During the field campaign there was no rainfall, however the area received a significant amount of rain (97 mm) in the 2 weeks prior to sampling. No surface runoff was present in Chowder Bay during field investigations even though surface runoff is known to occur following rain events. Average surface water temperature was 21.3 ± 0.1 ºC while wind speeds were on average 2.8 ± 0.2 m s^{-1} leading to an average gas transfer velocity of ~ 1.8 ± 0.4 m d^{-1}. Dissolved oxygen showed a diel cycle in the first half of the field campaign with higher values during the day and lower averages at night. However, this pattern was not apparent on the last two days of measurements (Figure 2). Salinity did not show a tidal trend and remained within a narrow range of 33.4 to 34.4 which illustrates the oceanic nature of the sampling location. pH showed typical oceanic values ranging from 8.05 to 8.20.

Concentrations of ^{222}Rn had several peaks but were not clearly aligned with tides. ^{222}Rn concentrations ranged from 5.6 to 15.9 Bq m^{-3} and averaged 12.2 ± 2.1 Bq m^{-3}. Similarly, CO_2, CH_4 and N_2O did not follow a tidal trend and the daily variability decreased towards the end of the time series as tidal amplitudes increased. The three greenhouse gases were above atmospheric equilibrium (~ 400 µatm for CO_2, 2 nM for CH_4 and 7 nM for N_2O), indicating the cove was a source of CO_2, CH_4 and N_2O to the atmosphere. Partial pressure of CO_2 varied from 402 to 465 µatm with an average of 434 ± 2 µatm. CH_4 ranged from 5.7 to 12.6 nM with an average of 9.1 ± 0.3 nM while average N_2O was 8.1 ± 0.1 nM.

3.2. Groundwater

Salinity in groundwater samples ranged from fresh (0.3) to saline (34.8) with an average of 18.1 ± 4.1. The average ^{222}Rn concentration was 358 ± 107 Bq m^{-3}, 29-fold higher than average surface water observations. The average CO_2, CH_4, and N_2O concentrations in groundwater were 3.5, 7.2, and 2.8 times higher than the average surface water concentrations (Table 1, Figure 3), indicating the possibility of groundwater as a source of greenhouse gases to the bay.

3.3 Flux estimates

The non-steady state ^{222}Rn mass balance model indicated that groundwater was discharging into the bay at an average rate of 8.7 ± 5.8 cm d^{-1} (Figure 4). Estimated diffusive fluxes from the sediment core incubation experiment were 9.3 Bq m^{-2} d^{-1} which was less than 15% of the advection rates from the mass balance, indicating groundwater advection is the major contributor of groundwater to the bay rather than diffusion. There were similar dissolved ^{226}Ra activities at low and high tide (average of 0.5 ± 0.1 Bq m^{-3}). The production of ^{222}Rn through the decay of ^{226}Ra was negligible as average radium concentrations were <5% of ^{222}Rn activities in surface water. Previous studies have also reported ^{226}Ra decay and sediment diffusion to be a minor component of the ^{222}Rn mass balance in coastal areas influenced by SGD (Burnett and Dulaiova, 2006; Sadat-Noori et al., 2015; Tait et al., 2016).

Average atmospheric evasion losses were calculated at 10.1 Bq m^{-2} d^{-1} while average losses from Chowder bay water mixing with the wider Harbour were estimate to be 38.2 Bq m^{-2} d^{-1}. The average piston velocity calculated by multiple methods available in the literature was 1.8 ± 0.4 m d^{-1} (Table 2). The highest piston velocity and consequently highest GHG evasion rates were estimated by formulation suggested by Borges et al., (2004) while the lowest piston velocity was estimated when the Wanninkhof & McGillis (1999) empirical equation was used. Average CO_2 evasion from surface water was calculated to be 2.29 ± 0.5 mmol m^{-2} d^{-1} while average CH_4 and N_2O evasion rates were 12.89 ± 3.05 and 1.23 ± 0.25 µmol m^{-2} d^{-1} (Table 2).

Using the calculated discharge rate, groundwater-derived CO_2 fluxes were estimated to be 5.02 ± 2.28 mmol m^{-2} d^{-1}, while the groundwater-derived CH_4 and N_2O fluxes were 5.63 ± 2.55 and 1.72 ± 0.78 µmol m^{-2} d^{-1}, respectively (Table 2, Table 3). These CO_2 and N_2O groundwater-derived fluxes were 2 and 1.5–fold larger than average surface water fluxes while groundwater CH_4 was about half of surface water fluxes.

4. Discussion

4.1. Submarine groundwater discharge

SGD rates based on the continuous ^{222}Rn measurements in Chowder Bay showed semi-diurnal variability which suggests tidal pumping as a potential driver of SGD overlapping fresh SGD (Figure 4). The average groundwater advection rate (8.7 ± 5.8 cm d^{-1}) was indicative of considerable amount of groundwater discharging and interacting with bay surface water. Previous studies have reported a direct link and a significant inverse

relationship between SGD and tidal height (Santos et al., 2011; Barnes et al., 2006; Bouillon et al., 2007; Call et al., 2015). Here, surface water ^{222}Rn had no clear relationship with water levels (Figure 5) indicating that tidal pumping was not the only mechanism driving ^{222}Rn dynamics. ^{222}Rn concentrations in surface water peaked on low-low tides (day of 19/11 and night of 21/11 in Figure 2) and increased on high-low tide showing that tidal pumping may have occurred during larger tides. A potential additional driver of ^{222}Rn was freshwater inputs from the upper Sydney Harbour, but this is unlikely because most of the upstream ^{222}Rn would degas and decay by the time it reaches the outer Harbour area where we made our observations.

The wide range of salinities (0.3 - 34.8) observed in groundwater samples supports the notion of groundwater and surface water mixing in the subterranean estuary beneath the beach. This mixing within the subterranean estuary may explain the lack of correlation between ^{222}Rn and salinity in groundwater samples (not shown) and suggests that combined marine (tidal pumping) and terrestrial (hydraulic gradient) forces drive SGD into the bay. Salinity often has little or no effect on radon concentrations in groundwater (Swarzenski, 2007; Burnett et al., 2007). Based on the morphology of the bay which is nestled between the harbour and steep hills, hydraulic gradient is assumed to also driver SGD. The wet conditions prior to measurements may have increased groundwater levels and related groundwater inputs. The ^{222}Rn versus salinity scatter plot displayed a significant negative correlation (Figure 5). This implies that terrestrial freshwater inputs were dominant rather than recirculated seawater. The zero salinity intercept from ^{222}Rn-salinity observations (143 ± 45 Bq m^{-3}) was about 50% of the average ^{222}Rn concentration in beach groundwater (285 ± 87 Bq m^{-3} excluding the high concentration outlier sample GW 7 in Table 1). Considering ^{222}Rn losses in surface water via decay and atmospheric evasion, the intercept further suggests that much of the ^{222}Rn was related to fresh rather than recirculated saline groundwater discharge to the bay.

The average ^{222}Rn concentration in groundwater samples was used as the endmember in the mass balance to calculate SGD. The error associated with using this average concentration (i.e. the standard error of all groundwater measurements) is propagated through the groundwater discharge calculations to highlight the uncertainty associated with this approach. Surface water runoff from storm water was not included in the mass balance because there was no visible surface flows into Chowder Bay over the course of the study. We suggest future studies use a combination of radioisotope tracers (radon and radium) along with comprehensive spatial and seasonal sampling to better identify water circulations

patterns within Sydney Harbour and fully separate the contribution of fresh SGD and recirculated seawater to total SGD.

4.2. Greenhouse gas dynamics

A series of recent studies have shown a direct link between surface water fCO_2, CH_4, and N_2O and groundwater exchange in coastal and estuarine systems (Wong et al., 2013; Santos et al., 2015; Call et al., 2015; Maher et al., 2015; O'Reilly et al., 2015). Here, surface water ^{222}Rn versus fCO_2 scatter plot did not show a significant correlation (Figure 6), indicating groundwater may not be the primary driver of fCO_2 in the Bay. However, the positive correlation between ^{222}Rn concentrations in surface water and CH_4 and N_2O implies that groundwater discharge may be driving these gases in surface waters (Figure 6). Any freshwater inputs from the wider estuary were unlikely to be an important driver of fCO_2 in Chowder Bay implied by the non-significant correlation between fCO_2 and salinity (Figure 7). Interestingly, both methane and nitrous oxide had stronger correlations with ^{222}Rn than with fCO_2. This may be related to CO_2 uptake by phytoplankton (Figure 8) driving fCO_2 concentrations on a diel cycle.

Salinity mixing plots imply that freshwater is a major source of CH_4 and N_2O to the bay surface waters (Figure 7). The positive correlation with ^{222}Rn, in spite of large scatter, implies that SGD was a source of these gases. The y intercept of the equation explaining CH_4 and N_2O versus ^{222}Rn correlation implies that in the absence of ^{222}Rn (i.e., SGD approaching zero) CH_4 would be 4.3 nM, which is higher than atmospheric equilibrium (2.1 nM) suggesting sources of CH_4 different than just SGD. However, the y intercept would be 7.3 nM for N_2O which is close to the average surface water observations (8.1 ± 0.1) and similar to atmospheric equilibrium concentrations of 7.3 nM, suggesting groundwater as the main source of N_2O. There was no direct rainfall during the field campaign, therefore upstream river inputs and urban runoff are inferred as the main additional sources of CH_4 and N_2O. The Parramatta River had higher than base flow conditions at the time of sampling due to a total rainfall of 54.8 mm distributed over the week prior to sampling. High flow conditions are associated with high amounts of total nitrogen being delivered to the Harbour by river flow (Hedge et al., 2014) and may be responsible for higher concentrations of N_2O being delivered into the Harbour.

If we use the surface water CH_4 and N_2O zero salinity intercepts from the regression equations of the mixing plots (CH_4 = 205 nM at zero salinity; N_2O = 37.8 nM at zero salinity)

and compare with the groundwater endmember we observed that surface water zero salinity intercepts were 3- and 2-fold higher, respectively, than the average beach groundwater concentrations. This indicates sources other than groundwater may drive the gases and/or some consumption of these gases occurs in the subterranean estuary. Estuarine surveys from the freshwater endmember to the mouth would help elucidate the role of upstream freshwater inputs of greenhouse gases to Sydney Harbour. When these zero salinity intercept concentrations are compared with river water endmember concentrations detected elsewhere, a close match is observed. A study on Brisbane River Estuary, Australia, with a water depth of 10 meters reported river CH_4 and N_2O concentrations to be 277 and 20 nM, respectively (Sturm et al., 2016), which were similar to the concentrations observed during this study. This supports the notion that a combination of SGD inputs and fresh surface water inputs from upstream may drive CH_4 and N_2O in Chowder Bay.

4.3. SGD-derived GHG fluxes

The water to air GHG fluxes showed that the bay was a source of CO_2 (2.29 mmol m^{-2} d^{-1}), CH_4 (12.89 μmol m^{-2} d^{-1}) and N_2O (1.23 μmol m^{-2} d^{-1}) to the atmosphere (Table 2). Chowder Bay had CO_2 evasion rates much lower than the average fluxes observed in other lower estuaries with salinities higher than 25 (23.83 mmol m^{-2} d^{-1}; Chen et al., 2013). For example, Maher et al. (2015) found average CO_2 fluxes of North Creek lower estuary, a subtropical tidal estuary located at NSW, Australia to be 10 mmol m^{-2} d^{-1}. Call et al. (2016) reported an average CO_2 evasion rate of 9.4 mmol m^{-2} d^{-1} at the mouth of a tidal estuary located at Southern Moreton Bay, QLD, Australia. Here, primary productivity consuming CO_2 and mixing with near atmospheric equilibrium shelf waters are probably the main cause for the lower than average CO_2 fluxes. The influence of tidal dilution can also be seen in Figure 2, whereas when tidal amplitude increases towards the end of the time series, there is lower variability in ^{222}Rn and GHG concentrations. This gradual increase of salinity could be a decrease in fresh groundwater discharge due to higher water levels (head) in the bay and/or a decrease in freshwater inputs to the wider Sydney Harbour.

Greenhouse gas concentrations in groundwater were much higher than those observed in the bay (Figure 3), resulting in a net greenhouse gas fluxes from groundwater to surface water and surface water to atmosphere (Table 3). The ^{222}Rn mass balance provided quantitative results to build on the interpretation from the correlation analysis. The estimated fluxes of groundwater-derived fluxes can account for 100% of the CO_2 and N_2O and 43% of the CH_4 surface water evasion fluxes, implying SGD was the major source of GHG to the Harbour.

There was however a significant wind event during sampling which produced maximum wind speeds up to 8.1 m s^{-1} leading to *k* values as high as 7.5 m d^{-1} which corresponded to a decrease in CH_4 and N_2O concentrations, but no obvious influence on fCO_2 or ^{222}Rn concentrations.

The reported high contribution of SGD to GHG evasion is related to groundwater discharge being confined to a narrow seepage face near the location where measurements were conducted. While no information on the width of the seepage face is available for Chowder Bay, investigations elsewhere have shown seepage faces in the range of 1-200 m (Taniguchi et al., 2003; Paytan et al., 2006; Santos et al., 2009). Therefore, while SGD inputs of GHGs may only occur in this narrow seepage face close to our sampling station, evasion to the atmosphere can occur over a much larger area (Sydney Harbour is about 1500 m wide near Chowder Bay). This may create a false perception that groundwater is important in the entire Harbour. Since our estimates are localized and representative of a small embayment only, more spatial and temporal sampling is required to investigate this hypothesis in the wider Sydney Harbour. However, these flux estimates associated with the correlation analysis support our initial hypothesis that SGD is an important source of greenhouse gases in Sydney Harbour embayments.

4.4 CO_2-equivalent GHG emissions

Different greenhouse gases have different global warming potentials. In order to compare the overall contribution of the different greenhouse gases, CH_4 and N_2O were converted to CO_2-equivalent emissions from the bay assuming a 20 and 100 year sustained-flux global warming potential (Figure 9). Over a 20-year time frame, CH_4 and N_2O are 96 and 250 times more potent to impact global warming compared to CO_2 on a mass basis (Neubauer and Megonigal, 2015). Over a 100-year time frame, CH_4 and N_2O are 45 and 270 times more potent to impact global warming compared to CO_2 on a mass basis (Neubauer and Megonigal, 2015). On a 20-year time frame the combined emissions of CH_4 and N_2O accounted for 25% of the total CO_2-equivalent emissions in surface water while on a 100-year time frame this was 19% (Figure 9). For SGD-derived fluxes, CH_4 and N_2O accounted for about 10% of CO_2-equivalent emissions. Therefore, not accounting for SGD-derived CH_4 and N_2O emissions could overlook an important transport pathway of greenhouse gases into receiving waters. Our approach combining measurements of these three greenhouses gases offers insights not only into their drivers, but may also help constraining local, regional and global greenhouse gas budgets.

5. Conclusion

We presented the first ^{222}Rn, carbon dioxide, methane and nitrous oxide surface water time series for a Sydney Harbour embayment (Chowder Bay). This is of importance for investigating the role of SGD on GHG emissions in urbanized aquatic environments. The results showed a significant amount of groundwater (8.7 ± 5.8 cm d^{-1}) was entering the bay as traced by ^{222}Rn. Chowder Bay was a source of greenhouse gases to the atmosphere even though water–air fluxes were smaller than similar systems. A radon mass balance suggested that SGD was a major source of greenhouse gases to the bay. Since our results are site specific, broader spatial and temporal coverage including the upper and middle parts of Sydney Harbour are required to better understand SGD rates and GHG dynamics in the Harbour.

Acknowledgements - We would like to thank Clinton Grosvenor for his contribution during field work, and staff from the Sydney Institute of Marine Science (SIMS) for their hospitality. IRS and DTM are funded through Australian Research Council DECRA Fellowships (DE140101733 and DE150100581). We acknowledge support from the Australian Research Council (DP120101645 and LE120100156).

References

Adame, M.F., Kauffman, J.B., Medina, I., Gamboa, J.N., Torres, O., 2013. Carbon stocks of tropical coastal wetlands within the karstic landscape of the Mexican Caribbean. PLoS ONE, 8 (2), http://dx.doi.org/10.1371/journal.pone.0056569.

Arévalo-Martínez, D. L., M. Beyer, M. Krumbholz, I. Piller, A. Kock, T. Steinhoff, A. Körtzinger, and H. W. Bange. 2013. A new method for continuous measurements of oceanic and atmospheric N_2O, CO and CO_2: performance of off-axis integrated cavity output spectroscopy (OA-ICOS) coupled to non-dispersive infrared detection (NDIR), Ocean Science, 9(6), 1071-1087.

Bange, H. W., S. Rapsomanikis, and M. O. Andreae. 1996. Nitrous oxide in coastal waters. Global Biogeochemical Cycles, 10(1), 197-207.

Banks, J.L., Hedge, L.H., Hoisington, C., Strain, E.M., Steinberg, P.D. and Johnston, E.L., 2016. Sydney Harbour: Beautiful, diverse, valuable and pressured. Regional Studies in Marine Science, doi:10.1016/j.rsma.2016.04.007

Barnes J., Ramesh R., Purvaja R., Nirmal Rajkumar A., Senthil Kumar B., Krithika K., Ravichandran K., Uher G. and Upstill- Goddard R. (2006) Tidal dynamics and rainfall control N_2O and CH_4 emissions from a pristine mangrove creek. Geophysical Research Letters, 33, L15405.

Beck, A.J., Cochran, J.K. and Sañudo-Wilhelmy, S.A., 2009. Temporal trends of dissolved trace metals in Jamaica Bay, NY: importance of wastewater input and submarine groundwater discharge in an urban estuary. Estuaries and Coasts, 32(3), 535-550.

Birch G. F. and Taylor S. E. 1999. Source of heavy metals in sediments of the Port Jackson estuary, Australia. Science of the Total Environment, 227, 123–138.

Birch, G.F., Cruickshank, B. and Davis, B., 2010. Modelling nutrient loads to Sydney estuary (Australia). Environmental Monitoring and Assessment, 167(1-4), 333-348.

Birch, G.F., Evenden, D. and Teutsch, M.E., 1996. Dominance of point source in heavy metal distributions in sediments of a major Sydney estuary (Australia). Environmental Geology, 28(4), 169-174.

Birch, G.F., Lean, J. and Gunns, T., 2015. Historic change in catchment land use and metal loading to Sydney estuary, Australia (1788–2010). Environmental Monitoring and Assessment, 187(9), 1-15.

Birch, G.F., McCready, S., Long, E.R., Taylor, S.S. and Spyrakis, G., 2008. Contaminant chemistry and toxicity of sediments in Sydney Harbour, Australia: spatial extent and chemistry–toxicity relationships. Marine Ecology Progress Series, 363, 71-87.

Borges, A., B. Delille, L.-S. Schiettecatte, F. Gazeau, G. Abril, and M. Frankignoulle. 2004. Gas transfer velocities of CO_2 in three European estuaries (Randers Fjord, Scheldt and Thames). Limnology and Oceanography, 49, 1630‑1641.

Borges, A.V. and Abril, G., 2011. Carbon Dioxide and Methane Dynamics in Estuaries. In: W. Editors-in-Chief: Eric and M. Donald (Editors), Treatise on Estuarine and Coastal Science, Academic Press, Waltham, pp. 119-161.

Bouillon, S., Middelburg, J.J., Dehairs, F., Borges, A.V., Abril, G., Flindt, M.R., Ulomi, S. and Kristensen, E. 2007. Importance of intertidal sediment processes and porewater exchange on the water column biogeochemistry in a pristine mangrove creek (Ras Dege, Tanzania). Biogeosciences, 4, 311–322.

Burnett, W.C. and Dulaiova, H., 2003. Estimating the dynamics of groundwater input into the coastal zone via continuous radon-222 measurements. Journal of Environmental Radioactivity, 69(1), 21-35.

Burnett, W.C., Dulaiova, H., 2006. Radon as a tracer of submarine groundwater discharge into a boat basin in Donnalucata, Sicily. Continental Shelf Research, 26, 862‑873.

Burnett, W.C., et al., 2006. Quantifying submarine groundwater discharge in the coastal zone via multiple methods. Science of Total Environment, 367 (2–3), 498–543.

513 Burnett, W.C., R.N. Peterson, I.R. Santos, and Hicks, R.W., 2010. Use of automated radon
514 measurements for rapid assessment of groundwater flow into Florida streams. Journal of
515 Hydrology, 380, 298‐304.
516 Burnett, W.C., Santos, I.R., Weinstein, Y., Swarzenski, P.W., Herut, B., 2007. Remaining
517 uncertainties in the use of Rn-222 as a quantitative tracer of submarine groundwater discharge,
518 in: Sanford, W., Langevin, C., Polemio, M., Povinec, P. (Eds.), A new focus on groundwater-
519 seawater interactions. IAHS Publication No 312, Perugia, Italy, pp. 109-118.
520 Burnett, W.C., Wattayakorn, G., Taniguchi, M., Dulaiova, H., Sojisuporn, P., Rungsupa, S. and
521 Ishitobi, T., 2007. Groundwater-derived nutrient inputs to the Upper Gulf of
522 Thailand. Continental Shelf Research, 27(2), 176-190.
523 Call, M., et al. 2015. Spatial and temporal variability of carbon dioxide and methane fluxes over semi-
524 diurnal and spring-neap-spring timescales in a mangrove creek. Geochimica et Cosmochimica
525 Acta, 150, 211‐225.
526 Charette, M. A., and M. C. Allen. 2006. Precision Ground Water Sampling in Coastal Aquifers Using
527 a Direct-Push, Shielded-Screen Well-Point System. Groundwater Monitoring and Remediation,
528 26, 87-93.
529 Chen, C.T.A., et al., 2013. Air–sea exchanges of CO_2 in the world's coastal seas. Biogeosciences, 10
530 (10), 6509–6544.
531 Crusius, J. and Wanninkhof, R., 2003. Gas transfer velocities measured at low wind speed over a
532 lake. Limnology and Oceanography, 48(3),1010-1017
533 Cyronak, T., I. R. Santos, D. V. Erler, D. T. Maher, and B. D. Eyre, 2014, Drivers of pCO2 variability
534 in two contrasting coral reef lagoons: The influence of submarine groundwater discharge,
535 Global Biogeochemical Cycles, 28, 398–414.
536 Das, A. P., Marchesiello, P., & Middleton, J. H., 2006. Numerical modelling of tide-induced residual
537 circulation in Sydney Harbour. Marine and Freshwater Research, 51, 97–112.
538 Dulaiova, H. and Burnett, W.C., 2006. Radon loss across the water-air interface (Gulf of Thailand)
539 estimated experimentally from ^{222}Rn-^{224}Ra. Geophysical Research
540 Letters, DOI: 10.1029/2005GL025023.
541 Gatland, J.R., I.R. Santos, D.T. Maher, T. Duncan, and D.V. Erler. 2014. Carbon dioxide and methane
542 missions from an artificially drained coastal wetland during a flood: Implications for wetland
543 global warming potential. Geophysical Research: Biogeosciences, 119, 1698‐1716.
544 Glasby, T.M., 2001. Development of sessile marine assemblages on fixed versus moving
545 substrata. Marine Ecology Progress Series, 215, 37-47.
546 Hatje, V., Apte, S.C., Hales, L.T. and Birch, G.F., 2003. Dissolved trace metal distributions in Port
547 Jackson Estuary (Sydney Harbour), Australia. Marine Pollution Bulletin, 46(6), 719-730.

548 Hatje, V., Rae, K. and Birch, G.F., 2001. Trace metal and total suspended solids concentrations in
549 freshwater: the importance of small-scale temporal variation. Journal of Environmental
550 Monitoring, 3(2), 251-256.
551 Hedge L. H., Johnston E. L., Ahyong S. T., Birch G. F., Booth D. J., Creese B. G., Doblin M.A.,
552 Figueira W. F., Gribben P. E., Hutchings P. A., Pritchard T. R., Marzinelli E. M., Steinberg P.
553 D., Roughan M. Sydney Harbour: A systematic review of the science. 2014. Sydney Institute of
554 Marine Science Technical Report.
555 Hill, N.A., Johnston, E.L., King, C.K. and Simpson, S.L., 2011. Physico-chemical changes in metal-
556 spiked sediments deployed in the field: Implications for the interpretation of in situ
557 studies. Chemosphere, 83(4), 400-408.
558 Johnston, E.L., Mayer-Pinto, M., Hutchings, P.A., Marzinelli, E.M., Ahyong, S.T., Birch, G., Booth,
559 D.J., Creese, R.G., Doblin, M.A., Figueira, W. and Gribben, P.E., 2015. Sydney Harbour: what
560 we do and do not know about a highly diverse estuary. Marine and Freshwater
561 Research, 66(12), 1073-1087.
562 Knee, K. and Paytan, A., 2011. Submarine groundwater discharge: A source of nutrients, metals, and
563 pollutants to the coastal ocean. Treatise on Estuarine and Coastal Science, 4, 205-234.
564 Lecher, A.L., Mackey, K., Kudela, R., Ryan, J., Fisher, A., Murray, J. and Paytan, A., 2015. Nutrient
565 loading through submarine groundwater discharge and phytoplankton growth in Monterey Bay,
566 CA. Environmental Science & Technology, 49(11), 6665-6673.
567 Lee, J.-M., and G. Kim. 2006. A simple and rapid method for analyzing radon in coastal and ground
568 waters using a radon-in-air monitor. Journal Environmental Radioactivity, 89219-228.
569 Lee, S.B., Birch, G.F. and Lemckert, C.J., 2011. Field and modelling investigations of fresh-water
570 plume behaviour in response to infrequent high-precipitation events, Sydney Estuary,
571 Australia. Estuarine, Coastal and Shelf Science, 92(3), 389-402.
572 Lovelock, C.E., Ruess, R.W., Feller, I.C., 2011. CO2 efflux from cleared mangrove peat. PLoS ONE
573 6, e21279. http://dx.doi.org/10.1371/journal.pone.0021279.
574 Ma, X., Zhang, G.L., Liu, S.M., Wang, L., Li, P.P., Gu, P.P. and Sun, M.S., 2016. Distributions and
575 fluxes of nitrous oxide in lower reaches of Yellow River and its estuary: Impact of water-
576 sediment regulation. Estuarine, Coastal and Shelf Science, 168, 22-28.
577 Maher, D.T., K. Cowley, I.R. Santos, P. Macklin, and B.D. Eyre. 2015. Methane and carbon dioxide
578 dynamics in a subtropical estuary over a diel cycle: insights from automated in situ radioactive
579 and stable isotope measurements. Marine Chemistry 168, 69‑79.
580 Maher, D.T., Santos, I.R., Leuven J.R., Oakes J.M., and Eyre, B.D. 2013. Novel use of cavity ring-
581 down spectroscopy to investigate aquatic carbon cycling from microbial to ecosystem scales.
582 Environmental Sciences & Technology, 47(22), 12938-12945.

583 Moore, W.S., 2003. Sources and fluxes of submarine groundwater discharge delineated by radium
584 isotopes. Biogeochemistry, 75‐93, 75‐93.
585 Moore, W.S., 2010. The effect of submarine groundwater discharge on the ocean. Annual Review of
586 Marine Sciences, 2, 59–88.
587 Neubauer, S.C. and Megonigal, J.P., 2015. Moving beyond global warming potentials to quantify the
588 climatic role of ecosystems. Ecosystems, 18(6), 1000-1013.
589 O'Reilly, C., Santos, I.R., Cyronak, T., McMahon, A., Maher, D.T., 2015. Nitrous oxide and methane
590 dynamics in a coral reef lagoon driven by pore water exchange: Insights from automated high-
591 frequency observations. Geophysical Research Letters, 42, 2885-2892.
592 Paytan, A., Shellenbarger, G.G., Street, J.H., Gonneea, M.E., Davis, K., Young, M.B. and Moore,
593 W.S., 2006. Submarine groundwater discharge: An important source of new inorganic nitrogen
594 to coral reef ecosystems. Limnology and Oceanography, 51(1), 343-348.
595 Peterson, R.N., Burnett, W.C., Dimova, N., Santos, I.R., 2009. Comparison of measurement methods
596 or radium-226 on manganese-fiber. Limnology and Oceanography: Methods, 7, 196–205.
597 Porubsky W. P., Weston N. B., Moore W. S., Ruppel C. and Joye S. B. 2014. Dynamics of submarine
598 groundwater discharge and associated fluxes of dissolved nutrients, carbon, and trace gases to
599 the coastal zone (Okatee River estuary, South Carolina). Geochimica Cosmochimica Acta, 131,
600 81–97.
601 Raymond, P.A. and Cole, J.J., 2001. Gas exchange in rivers and estuaries: Choosing a gas transfer
602 velocity. Estuaries and Coasts, 24(2), 312-317.
603 Sadat-Noori M, Maher D.T, Santos I.R. 2016. Groundwater Discharge as a Source of Dissolved
604 Carbon and Greenhouse Gases in a Subtropical Estuary. Estuaries and Coasts, 39, 639-656.
605 Sadat-Noori, M., Santos, I., Sanders, C., Sanders, L., Maher, D., 2015. Groundwater discharge into an
606 estuary using spatially distributed radon time series and radium isotopes. Journal of Hydrology,
607 528, 703–719.
608 Santos I. R., Eyre B. D. and Huettel M. 2012. The driving forces of porewater and groundwater flow
609 in permeable coastal sediments: a review. Estuaries, Coastal and Shelf Science, 98, 1–15.
610 Santos, I.R. and Eyre, B.D., 2011. Radon tracing of groundwater discharge into an Australian estuary
611 surrounded by coastal acid sulphate soils. Journal of Hydrology, 396(3), 246-257.
612 Santos, I.R., Beck, M., Brumsack, H.J., Maher, D.T., Dittmar, T., Waska, H. and Schnetger, B., 2015.
613 Porewater exchange as a driver of carbon dynamics across a terrestrial-marine transect: Insights
614 from coupled ^{222}Rn and pCO_2 observations in the German Wadden Sea. Marine Chemistry,
615 171, 10-20.
616 Santos, I.R., Burnett W.C., Dittmar T., Suryaputra I.G.N.A. and Chanton J. 2009. Tidal pumping
617 drives nutrient and dissolved organic matter dynamics in a Gulf of Mexico subterranean
618 estuary. Geochimica et Cosmochimica Acta, 73, 1325‐1339.

Siboni, N., Balaraju, V., Carney, R., Labbate, M. and Seymour, J.R., 2016. Spatiotemporal Dynamics of Vibrio spp. within the Sydney Harbour Estuary. Frontiers in Microbiology, 7: 460.

Smoothey, A.F., Gray, C.A., Kennelly, S.J., Masens, O.J., Peddemors, V.M. and Robinson, W.A., 2016. Patterns of Occurrence of Sharks in Sydney Harbour, a Large Urbanised Estuary. PLoS ONE, 11(1), p.e 0146911.

Stark, J.S., 1998. Heavy metal pollution and macrobenthic assemblages in soft sediments in two Sydney estuaries, Australia. Marine and Freshwater Research, 49(6), 533-540.

Stieglitz, T.C., Cook, P.G., Burnett, W.C., 2010. Inferring coastal processes from regional scale mapping of 222Radon and salinity: examples from the Great Barrier Reef, Australia. Journal of Environmental Radioactivity, 101 (7), 544–552.

Sturm, K., Grinham, A., Werner, U. and Yuan, Z., 2016. Sources and sinks of methane and nitrous oxide in the subtropical Brisbane River estuary, South East Queensland, Australia. Estuarine, Coastal and Shelf Science, 168, 10-21.

Swarzenski, P.W., 2007. U/Th series radionuclides as coastal groundwater tracers. Chemical Reviews 107, 663-674.

Tait, D. R., D. T. Maher, P. A. Macklin, and I. R. Santos. 2016. Mangrove pore water exchange across a latitudinal gradient, Geophysical Research Letters, 43(7), 3334-3341.

Taniguchi, M., Burnett, W.C., Dulaiova, H., Siringan, F., Foronda, J., Wattayakorn, G., Rungsupa, S., Kontar, E.A. and Ishitobi, T., 2008. Groundwater discharge as an important land-sea pathway into Manila Bay, Philippines. Journal of Coastal Research, 24(sp1), 15-24.

Taniguchi, M., Burnett, W.C., Smith, C.F., Paulsen, R.J., O'rourke, D., Krupa, S.L. and Christoff, J.L., 2003. Spatial and temporal distributions of submarine groundwater discharge rates obtained from various types of seepage meters at a site in the Northeastern Gulf of Mexico. Biogeochemistry, 66(1-2), 35-53.

Wanninkhof, R. 1992. Relationship between wind speed and gas exchange over the ocean. Journal of Geophysical Research: Oceans (1978–2012) 97: 7373-7382.

Wanninkhof, R. and McGillis, W.R., 1999. A cubic relationship between air-sea CO2 exchange and wind speed. Geophysical Research Letters, 26(13), 1889-1892.

Webb, J.R., Maher, D.T., Santos, I.R., 2016. Automated, in situ measurements of dissolved CO_2, CH_4, and $\delta^{13}C$ values using cavity enhanced laser absorption spectrometry: Comparing response times of air-water equilibrators. Limnology and Oceanography: Methods, 14, 323-337.

Weiss, R. F. 1974. Carbon dioxide in water and seawater: the solubility of a non-ideal gas. Marine Chemistry, 2: 203-215.

Weiss, R. F., and B. A. Price 1980. Nitrous oxide solubility in water and seawater, Marine Chemistry, 8(4), 347–359.

Weiss, R., and B. Price. 1980. Nitrous oxide solubility in water and seawater. Marine Chemistry, 8(4), 347-359.

Wiesenburg, D. a., and Guinasso N. L., 1979. Equilibrium solubilities of methane, carbon monoxide, and hydrogen in water and sea water. Journal of Chemistry Engineering Data, 24(4), 356-360.

Wong, W.W., Grace, M.R., Cartwright, I., Cardenas, M.R., Zamora, P., Cook, P., 2013. Dynamics of groundwater-derived nitrate and nitrous oxide in a tidal estuary from radon mass balance modelling. Limnology and Oceanography, 58, 1689-1706.

661 Table 1. Groundwater observations in Chowder Bay, Sydney, Australia.

Sample ID	Date	Latitude	Longitude	Salinity	pH	Temp (℃)	Depth (m)	^{222}Rn (Bq m^{-3})	CO_2 (µatm)	CH_4 (nM)	N_2O (nM)
*GW 1	18/11/2015	33.83844	151.2543	0.3	6.89	25.1	3.5	340.9	12312.9	8056.9	17.0
GW 2	19/11/2015	33.83853	151.2542	0.5	9.24	23.5	3.0	177.6	1260.2	97.7	13.7
GW 3	18/11/2015	33.83865	151.2540	0.9	8.75	22.9	2.5	144.6	2028.7	79.3	13.4
GW 4	18/11/2015	33.83856	151.2544	17.5	7.81	21.7	2.0	119.2	1761.5	53.8	12.9
GW 5	18/11/2015	33.83858	151.2543	20.9	7.93	21.5	1.8	164.5	1893.3	87.4	15.5
GW 6	18/11/2015	33.83856	151.2544	34.8	7.75	21.0	1.0	181.9	2638.3	59.2	29.6
GW 7	19/11/2015	33.83858	151.2543	28.9	7.49	20.8	1.5	1018.5	1490.9	54.1	27.4
GW 8	19/11/2015	33.83861	151.2544	22.6	7.76	22.4	1.7	867.8	1226.3	55.9	23.4
GW 9	19/11/2015	33.8386	151.2543	26.6	7.92	22.6	1.0	39.4	2280.7	53.4	23.4
GW 10	19/11/2015	33.83855	151.2543	28.6	7.84	23.7	1.0	525.6	1009.9	41.2	20.9
			Average	18.1	7.93	22.5		358.0	1732.2	64.7	19.7
			Std. dev.	13.1	0.65	1.3		338.2	535.6	18.8	6.0
			Std. error	4.1	0.2	0.4		106.9	169.3	6.2	1.9

662 *Outlier excluded from CO_2 and CH_4 averages.

663

664 Table 2. Greenhouse gas emmision from surface water calculated using multiple piston velocity (*k*) methods available in the literature.
665 Uncertainties indicate standard errors.

Equation	Average k (600/CO_2) (m d^{-1})	Average CO_2 Flux (mmol m^{-2} d^{-1})	Average CH_4 Flux (µmol m^{-2} d^{-1})	Average N_2O Flux (µmol m^{-2} d^{-1})	Reference
$K = 0.31U^2 (Sc/660)^{-1/2}$	1.4	1.79	9.90	0.93	Wanninkhof (1992)
$K = 0.228U^{2.2} + 0.168$	1.5	1.94	10.74	1.01	Crusius & Wanninkhof (2003)
$K = 0.0283U^3 (Sc/660)^{-1/2}$	0.8	1.07	5.82	0.53	Wanninkhof & McGillis (1999)
$K = 1.91e^{0.35u} (Sc/660)^{-1/2}$	2.4	3.05	17.33	1.65	Raymond & Coles (2001)
$K = 5.141u^{0.758} (Sc/660)^{-1/2}$	2.9	3.61	20.67	2.01	Borges et al. (2004)
Average	1.8±0.4	2.29±0.46	12.89±3.05	1.23±0.25	

666

667

668 Table 3. Groundwater advection rate and GW-derived GHG fluxes.

	Discharge rate ($cm\ d^{-1}$)	CO_2 ($mmol\ m^{-2}\ d^{-1}$)	CH_4 ($\mu mol\ m^{-2}\ d^{-1}$)	N_2O ($\mu mol\ m^{-2}\ d^{-1}$)
GW fluxes	8.7±5.8	5.02±2.28	5.63±2.55	1.72±0.78
Atmospheric evasion		2.29±0.46	12.89±3.05	1.23±0.25

669

670

671 Figure 1. Map of the study site in Chowder Bay, Sydney, Australia.

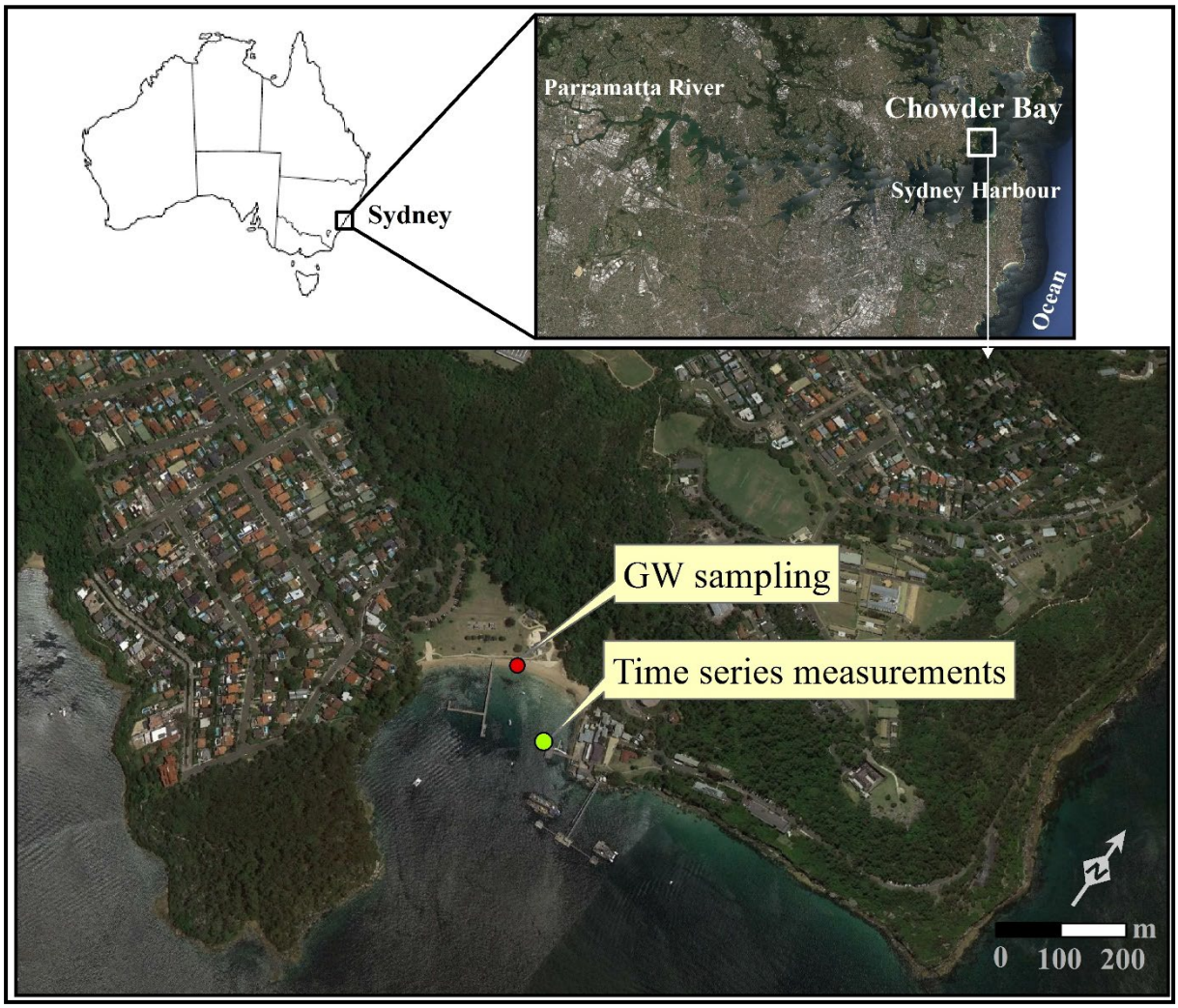

672

673

674 Figure 2. Time series of surface water physico-chemical parameters, ^{222}Rn and greenhouse
675 gases. Shaded areas indicate night time.

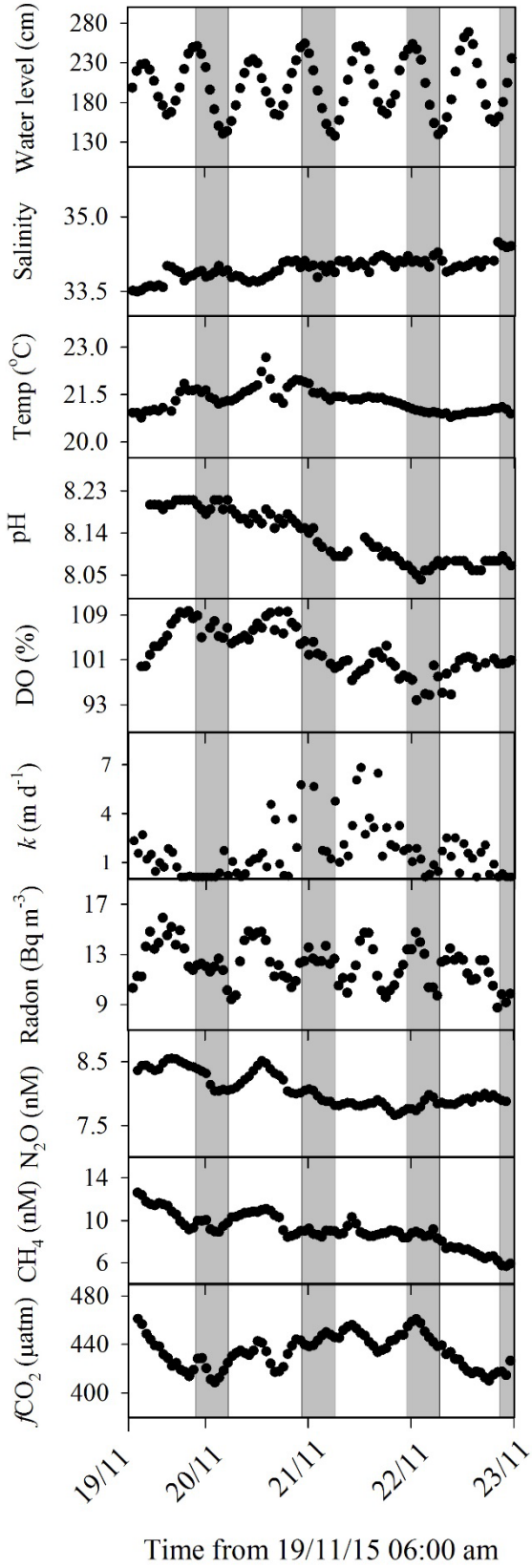

676

677 Figure 3. Groundwater to surface water ^{222}Rn and greenhouse gases ratios.

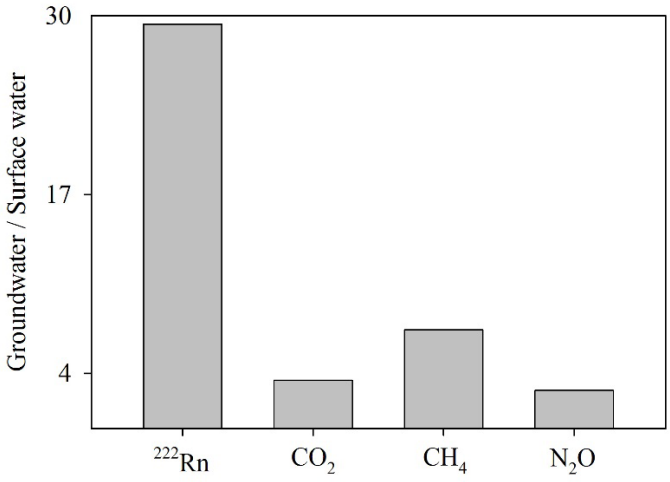

678

679

680 Figure 4. Groundwater advection rates over the study period. Error bars show propagated
681 uncertainties.

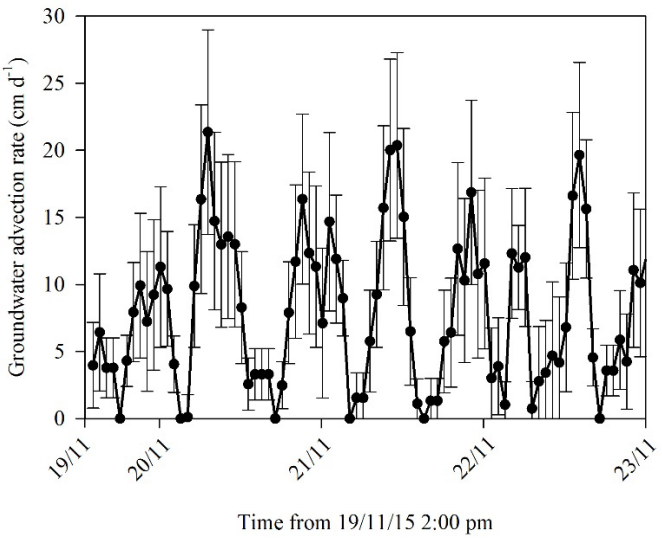

682

683 Figure 5. Surface water ^{222}Rn concentration versus depth and salinity.

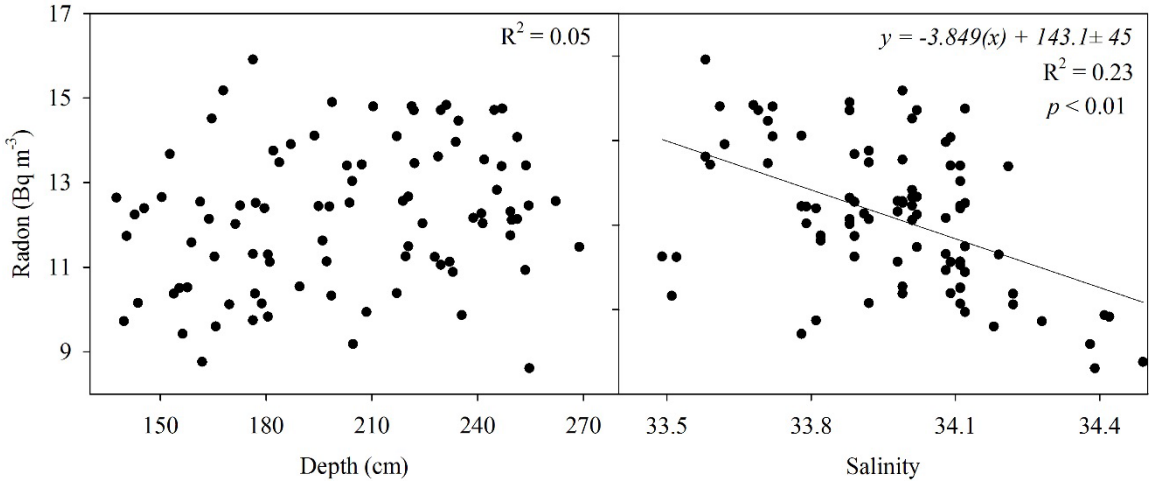

684

685 Figure 6. Surface water ^{222}Rn concentration versus greenhouse gas correlations.

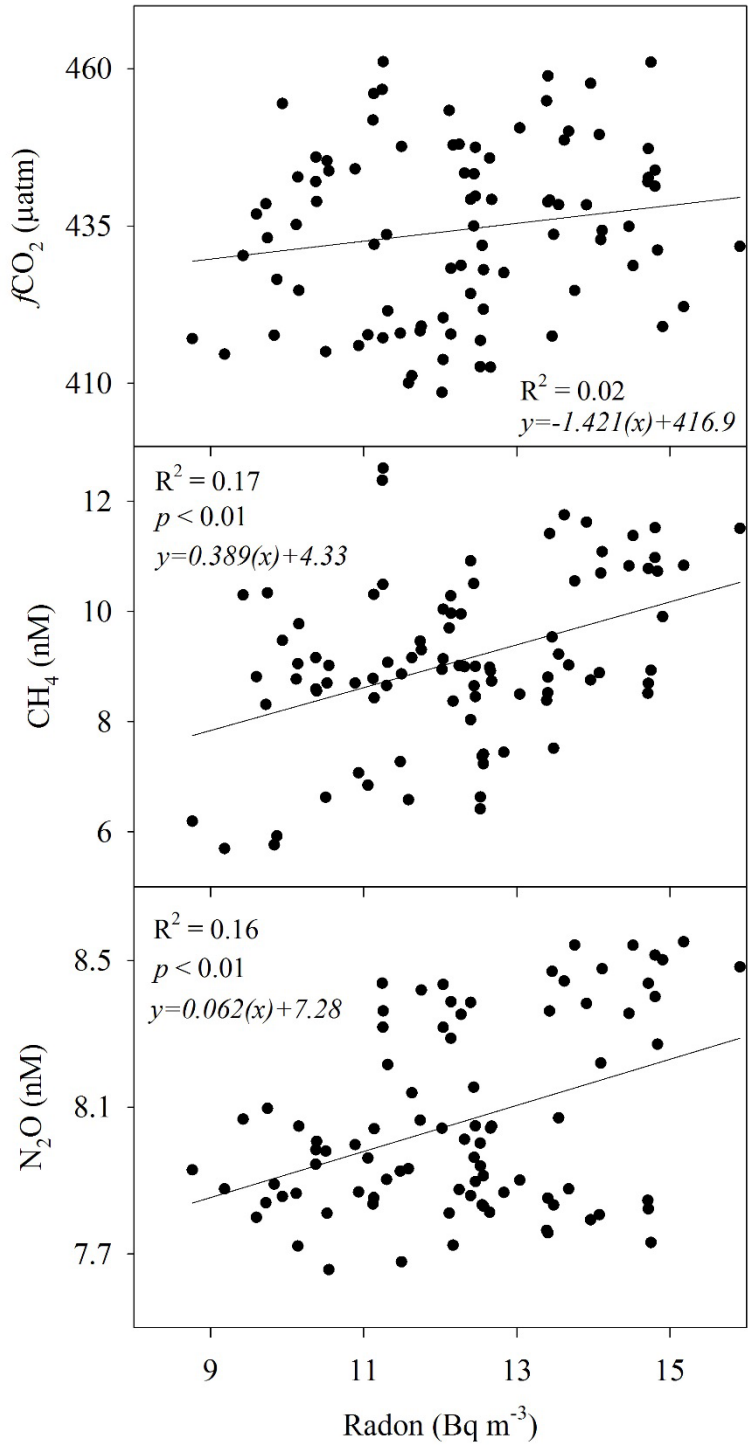

686

687 Figure 7. Greenhouse gases in surface and groundwater versus salinity indicating fresh
688 surface water is the primary source of GHG.

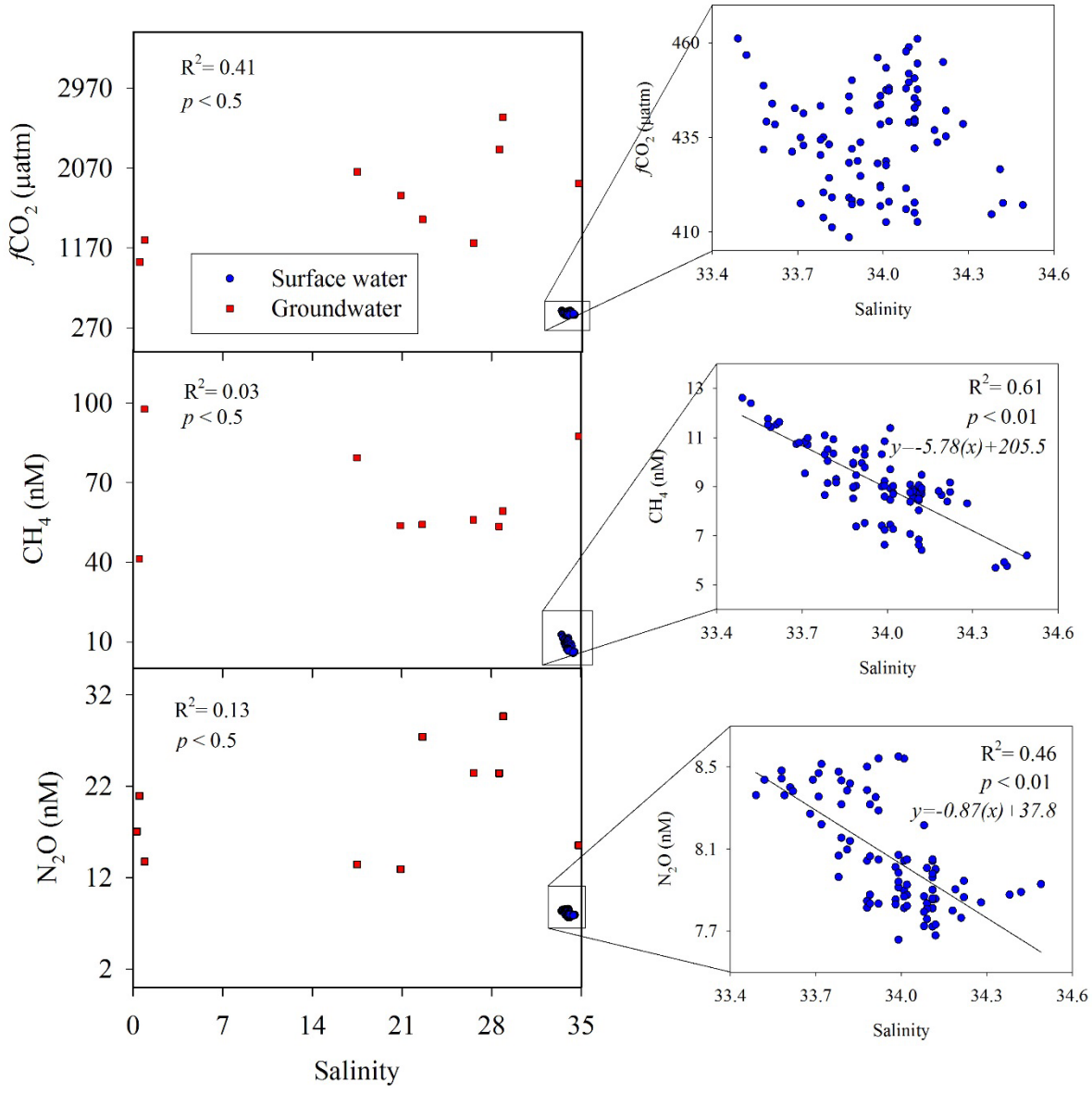

689

690 Figure 8. Fugacity of CO_2 and dissolved oxygen (% saturation) correlation indicating CO_2
691 uptake and release is regulated by photosynthesis.

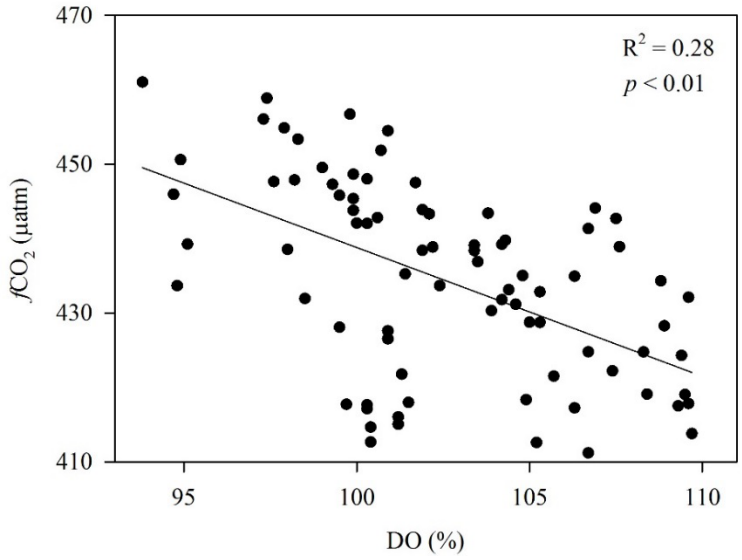

692

693

694 Figuer 9. The contribution of the three major greenhouse gases in CO_2 equilivants using the
695 20- and 100-year sustained-flux global worming potential of Neubauer and Megonigal
696 (2015).

697

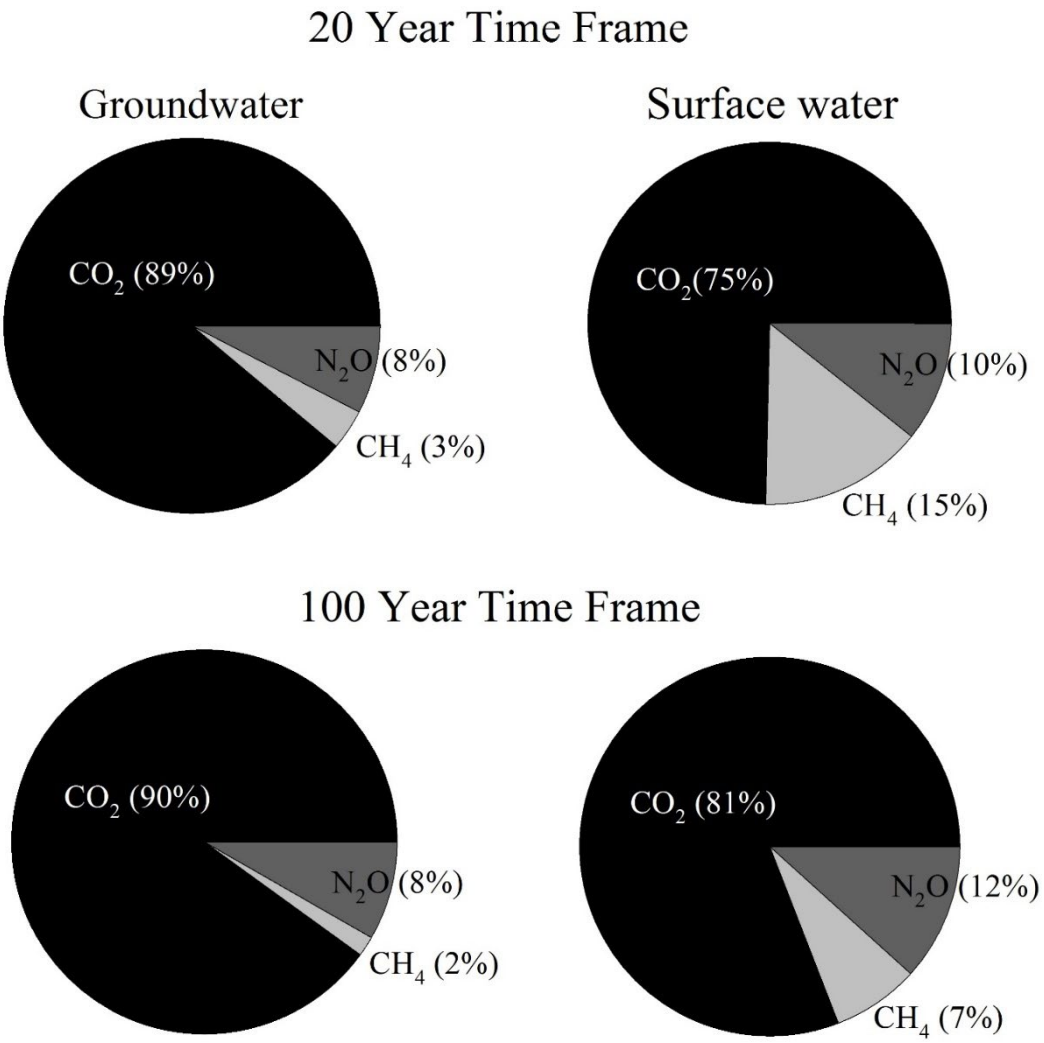

698

699